

SUPERNOVA NEUTRINOS, LSND AND MINIBOONE

MICHEL SOREL

Department of Physics, Columbia University, New York, NY 10027, USA

The unique constraints on neutrino oscillations which can be obtained by measuring the energy spectrum of supernova $\bar{\nu}_e$'s are first discussed. The focus is on 4-neutrino mass and mixing models capable of explaining the LSND evidence of $\bar{\nu}_\mu \rightarrow \bar{\nu}_e$ oscillations. The potential of the Fermilab neutrino detector MiniBooNE to observe supernova neutrinos is then addressed, and a general description of the detector is given. As of May, 2002, the MiniBooNE detector is fully operational.

1 Introduction

Supernovae (SNe) are extremely violent and luminous stellar explosions in which the optical luminosity of the star at maximum light emission can be as great as that of a small galaxy. There are two entirely different classes of SN explosions. SNe of type Ia are the cosmologically interesting ones, used as standard candles by cosmologists in their quest to understand the space-time structure of the Universe. SNe Ia are the most luminous optically, but do not have a significant neutrino emission. This presentation focuses exclusively on the other class of SNe, comprising the types II, Ib and Ic, which are known as “core-collapse” SNe.¹ Core-collapse SNe produce an intense and detectable neutrino burst emission.

In a core-collapse SN explosion, neutrinos and antineutrinos of all flavors are produced via: $NN \rightarrow NN\nu\bar{\nu}$, $e^+e^- \rightarrow \nu\bar{\nu}$, and other processes. Because of the very high matter density at the neutrino production site, neutrinos get trapped for some time and reach thermal equilibrium with the surrounding material. Neutrinos eventually escape over a typical timescale of 1 – 10 seconds and, ignoring neutrino oscillations, each flavor of neutrinos or antineutrinos would take away approximately the same fraction of energy, that is 1/6 of the total. However, the average neutrino energies at the neutrinospheres, *i.e.* the surfaces of last scattering for the neutrinos, differ from one flavor to another. The average energies are estimated to be 10 – 13MeV for ν_e , 14 – 17MeV for $\bar{\nu}_e$, 23 – 27MeV for $\nu_{\mu,\tau}, \bar{\nu}_{\mu,\tau}$.^{1,2}

There are several important reasons to try to detect neutrinos from core-collapse SNe on Earth. First, high-energy astrophysicists can better understand the complex core-collapse explosion mechanism itself, by looking at its neutrino emission. This is because about 99% of the gravitational binding energy liberated in a SN explosion, $\sim 3 \cdot 10^{53}$ erg, is emitted under the form of neutrinos. Second, given the much smaller neutrino cross-sections in the SN mantle compared to the photon cross-sections, neutrinos from a SN explosion reach Earth on the order of a few hours before the corresponding optical signature. An early warning could then be sent to astronomers, and the early stages of the optical SN explosion be observed. Finally, SN neutrinos provide an additional (and, in some respects, unique) handle for particle-physicists to discern neutrino masses and mixing.

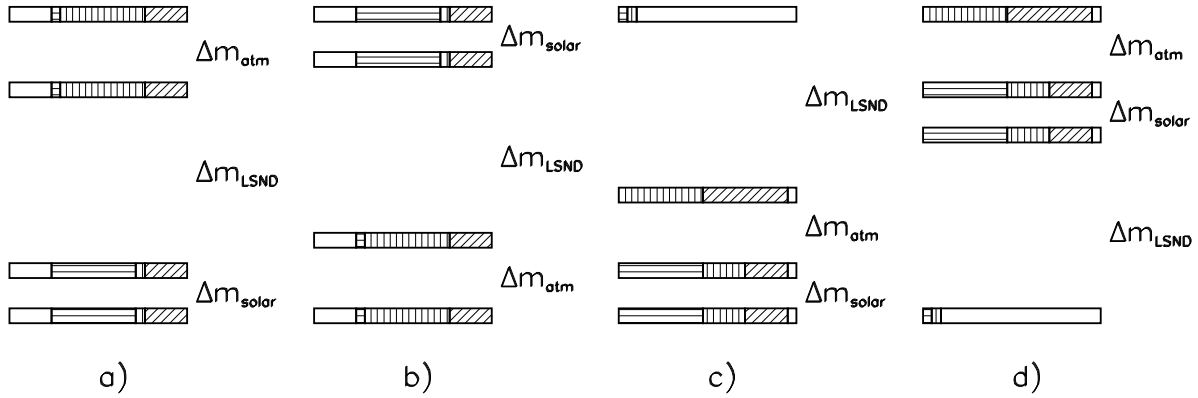


Figure 1: Flavor content of the four neutrino mass eigenstates for four 4-neutrino models. Masses increase from bottom to top. Empty rectangles: $\bar{\nu}_s$, horizontally-hatched: $\bar{\nu}_e$, vertically-hatched: $\bar{\nu}_\mu$, diagonally-hatched: $\bar{\nu}_\tau$. a) normal (2 + 2) model; b) LSND-inverted (2 + 2); c) normal (3 + 1); d) LSND-inverted (3 + 1). See text for the definition of “LSND-inverted” hierarchy.

The paper is organized as follows. In Section 2, the observation of SN $\bar{\nu}_e$ energy spectra as a probe for neutrino oscillations is discussed. The focus is on 4-neutrino mass and mixing models explaining the LSND evidence for $\bar{\nu}_\mu \rightarrow \nu_e$ oscillations. See Ref.³ for more details. Section 3 describes the MiniBooNE detector located at Fermilab, discussing in some detail its SN neutrino detection potential. Ref.⁴ gives more details on MiniBooNE as a SN neutrino detector.

2 Supernova neutrino energy spectra as a probe for neutrino oscillations

The SN models predictions for the neutrino energy spectra at production can be confronted with the observation of the SN $\bar{\nu}_e$ energy spectrum detected on Earth. In this section, the focus is on antineutrino oscillations (as opposed to neutrino oscillations) since the $\bar{\nu}_e$ detection on Earth is the easiest, as demonstrated for example for MiniBooNE in Section 3. Neutrino oscillations are expected to modify the spectrum since $\langle E_{\bar{\nu}_e} \rangle < \langle E_{\bar{\nu}_\mu, \bar{\nu}_\tau} \rangle$. The energy-dependence of the neutrino cross-section in the detector material⁵, approximately $\sigma_{\bar{\nu}_e p} \propto (E_{\bar{\nu}_e} - 1.29 \text{ MeV})^2$, helps in making the $\bar{\nu}_e$ energy spectrum distortion a sensitive experimental probe to neutrino oscillations. Quite interestingly, the extent of the spectrum modification depends crucially on the specifics of the neutrino mixing scheme and on the neutrino mass hierarchy under consideration.

2.1 4-neutrino models to explain neutrino oscillations

As it is well-known, we now have three experimental hints pointing toward neutrino oscillations: solar, atmospheric, and LSND oscillations. While the first two signatures are considered to be well-established, the LSND signal⁶ needs verification and should be definitely confirmed or refuted by the MiniBooNE experiment at Fermilab (see Section 3 and Ref.⁷). Assuming CPT-invariance, in order to explain all of the data via oscillations, (at least) four neutrinos are needed. In these 4-neutrino models, a *sterile* neutrino $\bar{\nu}_s$ with no standard weak couplings is added to the three *active* neutrino flavors $\bar{\nu}_e, \bar{\nu}_\mu, \bar{\nu}_\tau$. Apart from MiniBooNE, a “neutrino factory” as currently foreseen should also be able to distinguish 4-neutrino models from 3-neutrino ones, that is neutrino models without a sterile state.⁸

4-neutrino models fall into two categories: either (2 + 2), or (3 + 1) models. The flavor content of the four neutrino mass eigenstates involved in these models are shown in Fig.1. In (2 + 2) models, Figs.1a and b, the doublet of mass eigenstates responsible for solar oscillations and the doublet responsible for atmospheric neutrino oscillations are widely separated by the

LSND mass gap. In $(3+1)$ models, Figs.1c and d, the triplet of mass eigenstates responsible for solar and atmospheric oscillations and an almost entirely sterile state are separated by the LSND mass gap. Moreover, given the present experimental input on neutrino oscillations from shot-baseline experiments, we have no information about the sign of the mass difference Δm_{LSND} explaining LSND oscillations. Therefore, in addition to the “normal” hierarchies depicted in Figs.1a and c, we consider also the “LSND-inverted” hierarchies of Figs.1b and d, obtained from the normal ones by substituting $\Delta m_{LSND} \rightarrow \Delta m_{LSND}$.

2.2 Matter effects and oscillations in the supernova environment

In matter, $\bar{\nu}_e$ ’s undergo coherent CC forward-scattering from electrons, while all active flavors $\bar{\nu}$ ’s undergo coherent NC forward-scattering from electrons, protons, and neutrons. These processes give rise to an interaction potential $V = V_W + V_Z$, which has to be added to the Hamiltonian H_0 describing neutrino propagation in vacuum. In the flavor basis, we can write the Hamiltonian describing neutrino propagation in matter as:⁹

$$(H)_{\alpha\beta} = (H_0 + V)_{\alpha\beta} = U_{\alpha i}^* U_{\beta i} \frac{m_i^2}{2p} + A_\alpha \frac{G_F \rho}{m_N} \delta_{\alpha\beta} \quad (1)$$

where U is the mixing matrix relating the neutrino mass eigenstates $\bar{\nu}_i$ to the flavor eigenstates $\bar{\nu}_\alpha$, $\alpha = e, \mu, \tau, s$, via $|\bar{\nu}_\alpha\rangle = U_{\alpha i} |\bar{\nu}_i\rangle$, m_i is the mass of the neutrino mass eigenstate $\bar{\nu}_i$, p is the neutrino momentum, A_α is a flavor-dependent numerical coefficient which can be calculated³ and gives $A_\mu > A_\tau > A_s > A_e$, G_F is the Fermi constant, ρ is the matter density, and m_N is the nucleon mass. In Eq.1, we have neglected a term proportional to the identity matrix, since it is irrelevant for neutrino oscillations.

At the neutrinosphere, the matter density is so high ($\rho \sim 10^{12} \text{g/cm}^3$) that the interaction potential V dominates over the vacuum Hamiltonian H_0 , so that the propagation eigenstates coincide with the flavor eigenstates. As the propagation eigenstates free-stream outwards, toward regions of lower density in the SN environment, their flavor composition changes, ultimately reaching the flavor composition of the mass eigenstates in the vacuum. Given that neutrinos escape the SN as mass eigenstates, no further flavor oscillations occur on their path to the Earth. Therefore, flavor oscillations can occur: the probability $p_{\alpha \rightarrow \beta}$ for a state born as a $\bar{\nu}_\alpha$ to reach Earth behaving as a $\bar{\nu}_\beta$ is nonzero for $\alpha \neq \beta$. These probabilities $p_{\alpha \rightarrow \beta}$ can be calculated³ for all flavor combinations ($\alpha, \beta = e, \mu, \tau, s$), given a certain neutrino mixing matrix and hierarchy, and using the *adiabatic approximation*. Antineutrinos propagate adiabatically if the varying matter density they encounter changes slowly enough so that transitions between local (instantaneous) Hamiltonian eigenstates can be neglected throughout the entire antineutrino propagation. From these probabilities, one finds that the inverted schemes in Figs.1b and d predict large $\bar{\nu}_{\mu,\tau} \rightarrow \bar{\nu}_e$ conversions, and therefore large distortions to the $\bar{\nu}_e$ energy spectrum observed on Earth. On the contrary, the normal schemes in Figs.1a and c predict little distortions to the $\bar{\nu}_e$ spectrum caused by oscillations.

2.3 Application: constraints on oscillations from SN1987A

On Feb 23rd, 1987, SN1987A exploded in the Large Magellanic Cloud, a small satellite galaxy of the Milky Way. Its neutrino emission was detected by at least two neutrino detectors: Kamiokande-2 in Japan, and IMB-3 in the US. Overall, twenty neutrino interactions were detected, all of which consistent with $\bar{\nu}_e$ interactions.¹⁰ From the measured energy spectrum, a low-energy flux $F_{\bar{\nu}_e}$ was inferred, consistent with no oscillations. If we define the primary fluxes at production for $\bar{\nu}_\mu$ (or, equivalently, $\bar{\nu}_\tau$) and $\bar{\nu}_e$ as $F_{\bar{\nu}_\mu}^0$ and $F_{\bar{\nu}_\tau}^0$ respectively, and the *permutation factor* p as the high-energy admixture in the flux on Earth $F_{\bar{\nu}_e}$ due to $\bar{\nu}_{\mu,\tau} \rightarrow \bar{\nu}_e$ oscillations:

$$F_{\bar{\nu}_e}(E) \propto (p F_{\bar{\nu}_\mu}^0(E) + (1-p) F_{\bar{\nu}_e}^0(E)) \quad (2)$$

a conservative upper limit of $p < 0.22$ at 99% CL can be assumed.³

In conclusion, based on SN1987A neutrino data only, the inverted hierarchies of Figs.1b and d are excluded. On the other hand, for the normal mass hierarchy schemes in Figs.1a and c, SN1987A data do not provide competitive constraints with respect to existing constraints from reactor, accelerator, atmospheric and solar neutrinos; additional experimental input is necessary to unambiguously discern the neutrino mass and mixing properties. Undoubtedly, the detection of supernova neutrinos by present or near-term experiments such as MiniBooNE would prove very useful in this respect.

3 The MiniBooNE detector and its potential for detecting supernova neutrinos

3.1 Main motivation of the MiniBooNE experiment

The MiniBooNE experiment located at Fermilab is designed to be a definitive investigation of the LSND evidence for $\bar{\nu}_\mu \rightarrow \bar{\nu}_e$ oscillations, which is the first accelerator-based evidence for oscillations. The detector consists of a 12m diameter spherical tank covered on the inside by 1280 20cm diameter phototubes in the detector region and by 240 phototubes in the $> 99\%$ efficient veto region. The tank is filled with 0.8ktons of pure mineral oil, giving a fiducial volume mass of 0.44ktons. The detector is located 500m downstream of a new neutrino source that is fed by the 8GeV proton Booster. A 50m decay pipe following the Be target and magnetic focusing horn allows secondary pions to decay into ν_μ 's with an average energy of about 1GeV. By switching the horn polarity, a beam that is predominantly $\bar{\nu}_\mu$'s can be produced. An intermediate absorber can be moved into and out of the beam at a distance of 25m, to allow a systematic check of the backgrounds. With $5 \cdot 10^{20}$ protons on target (about a year at design intensity), MiniBooNE will be able to cover the entire LSND allowed region with high sensitivity ($> 5\sigma$). As of May, 2002, the detector is fully operational. High-intensity beam data-taking will start in July, 2002.

3.2 MiniBooNE as a supernova neutrino detector

This section is heavily borrowed from Ref⁴. MiniBooNE can also be used as a SN neutrino detector without interfering with the main accelerator-based oscillation search. This is because the Booster beam will operate with a duty factor of $8 \cdot 10^{-6}$; for the rest of the time, MiniBooNE will be functioning as a SN neutrino detector. Given the requirements for the accelerator-based search, the MiniBooNE detector was built with a dirt overburden of only 3m. This is enough to nearly eliminate the hadronic component in cosmic rays, and setting the total cosmic-ray muon rate in the detector at the level of 10kHz, with about 8kHz throughgoing and 2kHz stopping. Despite the likely skepticism, it has been shown a surface-level detector such as MiniBooNE can reduce its cosmic-ray muon backgrounds enough to function as a SN neutrino detector.⁴

The SN neutrino detection reaction in MiniBooNE is $\bar{\nu}_e + p \rightarrow e^+ + n$. The positrons will be detected in MiniBooNE by their Cherenkov (and scintillation) light. The neutrons will be radiatively captured on protons, but the resulting 2.2MeV gamma rays will not be visible, due to low-energy radioactivity backgrounds. The expected⁴ number N of events in MiniBooNE from a galactic SN explosion, at a distance $D = 10\text{kpc}$ and releasing a gravitational binding energy $E_B = 3 \cdot 10^{53}\text{erg}$, is $N \simeq 230$. This number assumes that all events within a radius of 5.5m from the center of the detector can be used, corresponding to a detector mass of 0.595ktons. The next-most important reaction in the detector will be the NC nuclear excitation of ^{12}C , which yields a 15.11MeV gamma, with only $N \simeq 30$ events expected⁴ and probably beyond reach.

In addition to detect as many SN neutrinos as possible, it is also desirable to measure the energy of the corresponding positrons accurately. Neglecting nuclear recoil, the relation between positron energy and neutrino energy is very simple: $E_{e^+} = E_{\bar{\nu}_e} - 1.29\text{MeV}$. One of the motivations for measuring the positron (and, therefore, neutrino) energy is given in Section 2,

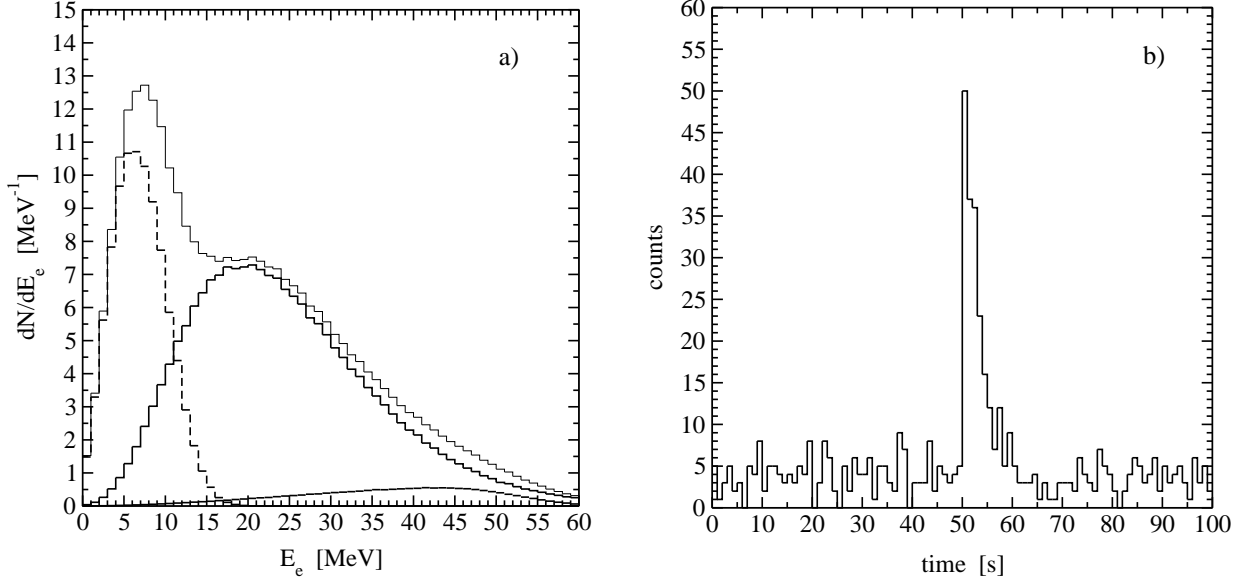


Figure 2: a) Spectra of the supernova signal (solid histogram peaking at 20MeV), ^{12}B decay background (dashed histogram peaking at low energy), and surviving muon decay background (solid histogram peaking at about 50MeV) in MiniBooNE versus the true positron total energy E_e , over a 10s interval assumed to contain the supernova signal. The thin solid histogram indicates the spectrum summed over signal and backgrounds. Detector deadtime and energy resolution are taken into account. Below about 5MeV, backgrounds from natural radioactivity will dominate over the spectra shown. b) Total number of signal and background events, in 1s bins over 100s, showing the Poisson fluctuations for one random simulated experiment with a supernova at $t = 50$ s. The background rate shown is after the cuts described in the text. The supernova signal was modeled as a sharp rise followed by an exponential decay with time constant of 3s.

that is to constrain neutrino oscillations. The relative energy resolution in MiniBooNE should be $\delta/E \simeq 0.75/\sqrt{E}$, where all energies are in MeV, and therefore reasonably good even at low, ~ 20 MeV, SN energies.

The key question, of course, is whether these signal events can be separated from the cosmic-ray related backgrounds expected in MiniBooNE. The two main backgrounds in the energy window of interest for SN neutrino detection are due to cosmic-ray muons decaying at rest, and to cosmic-ray muons capturing on ^{12}C nuclei followed by the beta decay of the resulting ^{12}B nuclei. The first background is due to Michel electrons, and can be reduced dramatically by imposing a holdoff of $15.2\mu\text{s}$ after every muon (the muon lifetime is $2.2\mu\text{s}$). With this holdoff, all but a 10^{-3} fraction of Michel decays are cut, so that the true rate of surviving Michels will be a small 2Hz in the main detector volume. The holdoff introduces a manageable deadtime fraction of 0.15. The second background is due to β^- -decay of ^{12}B nuclei. This decay has a very long lifetime of 20ms, and therefore a holdoff cannot be used. The rate for this background, integrated over all electron energies, is about 11Hz. However, most of the ^{12}B -decay electrons will have energies well below the typical SN event energies. Background rates from radioactive sources are negligible by cutting < 5 MeV events. The correctly normalized energy spectra for a galactic SN signal and for the two main backgrounds considered are shown in the Fig.2a taken from Ref.⁴, where the energy resolution of the MiniBooNE detector is also taken into account.

In sum, by cutting events below 10MeV, all of the backgrounds due to natural radioactivity and $\simeq 80\%$ of the ^{12}B decay background can be cut. The steady-state, background, rate should be about 4Hz. A candidate SN can be flagged by a large increase in the data rate, as shown in the Fig.2b, also taken from Ref.⁴.

What can MiniBooNE add to the worldwide effort¹¹ to detect SN neutrinos? First, it is highly desirable to have as many different detectors as possible. This will allow important cross checks of

the results. Second, MiniBooNE may be able to act as a node in the SuperNova Early Warning System (SNEWS). Having many independent nodes in the network greatly reduces the false alarm rate. Third, not all detectors are live all the time, due to upgrades and calibrations. Until Super-Kamiokande is being repaired, the $\bar{\nu}_e + p \rightarrow e^+ + n$ in MiniBooNE would be comparable to that from other detectors with hydrogen targets.

4 Summary

The phenomenology and observation of supernova neutrinos is an interdisciplinary topic, of interest to astronomers, high-energy astrophysicists, particle physicists. From the particle physics point of view, the observation of supernova neutrinos can provide unique constraints on the neutrino mass and mixing schemes explaining neutrino oscillations. The relation between the measured $\bar{\nu}_e$ energy spectra and various 4-neutrino models explaining the solar, atmospheric and LSND signatures for neutrino oscillations was discussed.³

Moreover, the supernova neutrino detection capabilities of the MiniBooNE detector were specifically addressed.⁴ It was shown that, despite being optimized for higher energies and being at a shallow depth of only 3m, the MiniBooNE detector can in principle clearly separate the neutrino signal expected from a galactic supernova explosion from the cosmic-ray related backgrounds. This extra-capability of the MiniBooNE detector causes no disruption to its main accelerator-based $\nu_\mu \rightarrow \nu_e$ search.

Acknowledgments

I am particularly indebted to Janet Conrad, Matthew Sharp, John Beacom and Joseph Formaggio, for the suggestions and help provided in preparing these proceedings, and to the Organizing Committee for the stimulating atmosphere of the 37th Rencontres de Moriond on Electroweak Interactions and Unified Theories.

References

1. G. G. Raffelt, Nucl. Phys. Proc. Suppl. **110**, 254 (2002) [arXiv:hep-ph/0201099].
2. H. T. Janka, In **Vulcano 1992, Proceedings, Frontier objects in astrophysics and particle physics** 345-374.
3. M. Sorel and J. Conrad, arXiv:hep-ph/0112214.
4. M. K. Sharp, J. F. Beacom and J. A. Formaggio, arXiv:hep-ph/0205035.
5. P. Vogel and J. F. Beacom, Phys. Rev. D **60**, 053003 (1999) [arXiv:hep-ph/9903554].
6. A. Aguilar *et al.* [LSND Collaboration], Phys. Rev. D **64**, 112007 (2001) [arXiv:hep-ex/0104049].
7. A. Bazarko [MiniBooNE Collaboration], Nucl. Phys. Proc. Suppl. **91**, 210 (2000) [arXiv:hep-ex/0009056].
8. D. Meloni, arXiv:hep-ph/0204351.
9. B. Kayser, arXiv:hep-ph/0104147.
10. M. Koshiba, Phys. Rept. **220**, 229 (1992).
11. J. F. Beacom and P. Vogel, Phys. Rev. D **58**, 053010 (1998) [arXiv:hep-ph/9802424]; J. F. Beacom and P. Vogel, Phys. Rev. D **58**, 093012 (1998) [arXiv:hep-ph/9806311]; L. Cadonati, F. P. Calaprice and M. C. Chen, Astropart. Phys. **16**, 361 (2002) [arXiv:hep-ph/0012082]; P. Vogel, arXiv:nucl-th/0111016; W. Fulgione [LVD Collaboration], Nucl. Phys. Proc. Suppl. **70**, 469 (1999); F. Halzen, J. E. Jacobsen and E. Zas, Phys. Rev. D **53**, 7359 (1996) [arXiv:astro-ph/9512080].